REPORT DOCUMENTATION PAGE

AFRL-SR-AR-TR-04-

0546

1. REPORT DATE (DD-MM-YYYY)	2. REPORT TYPE	3. DATES COVERED (From - To)
15-10-04	Final Technical Report	1 Sep 2003 - 30 Aug 2004

4. TITLE AND SUBTITLE

Adaptive Sensing and Control for Flexible Transmission in a Turbulent Medium

Adaptive Laser Beam Control Using Return Photon Statistics

5a. CONTRACT NUMBER
F49620-03-C-0054

5b. GRANT NUMBER
xxx

5c. PROGRAM ELEMENT NUMBER
0001AE

5d. PROJECT NUMBER
xxx

5e. TASK NUMBER
xxx

5f. WORK UNIT NUMBER
xxx

6. AUTHOR(S)
Gordon Lukesh
Susan Chandler

7. PERFORMING ORGANIZATION NAME(S) AND ADDRESS(ES)

Nukove Scientific Consulting
PO Box 2756
69 Vista Linda Rd
Ranchos de Taos, NM 87557

New Mexico State University
MSC 3-0
PO Box 30001
Las Cruces, NM 88003-8001

8. PERFORMING ORGANIZATION REPORT NUMBER
NSC0005

9. SPONSORING / MONITORING AGENCY NAME(S) AND ADDRESS(ES)
AFOSR
4015 Wilson Blvd - Room 713
Arlington, VA 22203-1954

NM

10. SPONSOR/MONITOR'S ACRONYM(S)
xxx

11. SPONSOR/MONITOR'S REPORT NUMBER(S)
xxx

12. DISTRIBUTION / AVAILABILITY STATEMENT
Approved for public release, distribution unlimited

20041105 146

13. SUPPLEMENTARY NOTES
none

14. ABSTRACT
Report developed under STTR contract for AF03T008. This Final Report details efforts under a Phase I Grant directed at taking an existing laser system pointing tool developed by Nukove and determining the feasibility of converting it into a real-time tool for eventual field work. Feasibility has been shown through the development of RHINO (Real-time Histogram Interpretation of Numerical Observations). RHINO shows that eventual field data may be streamed in and analyzed. Pointing estimates are available after 25 shots. As a prime example of the utility and feasibility, estimates of boresight will be available to adaptively control pointing with a goal of boresight reduction via feedback. Parallel to the software and modeling, New Mexico State University developed a laboratory testbed to emulate ground-to-space laser pointing systems. Data from the testbed was analyzed with RHINO and estimates concurred with the testbed inputs extremely well. The efforts resulted in three conference presentations and associated papers.

15. SUBJECT TERMS
STTR Report, pointing, jitter, boresight, RHINO, real-time, feedback

16. SECURITY CLASSIFICATION OF:			17. LIMITATION OF ABSTRACT	18. NUMBER OF PAGES	19a. NAME OF RESPONSIBLE PERSON
a. REPORT	b. ABSTRACT	c. THIS PAGE			Gordon Lukesh
Unclassified	Unclassified	Unclassified	none	25	19b. TELEPHONE NUMBER (include area code) 505 758 0169

Adaptive Sensing and Control for Flexible Transmission in a Turbulent Medium

Adaptive Laser Beam Control Using Return Photons Statistics

Final Report
AF03008

Contract #F49620-03-C-0054

Gordon Lukesh & Susan Chandler
Nukove Scientific Consulting
Ranchos de Taos, NM 87557

TABLE OF CONTENTS

LIST OF FIGURES

LIST OF ACRONYMS

AIT	- Active Imaging Testbed
AMOS	- Air Force Maui Optical Site
DAQ	- Digital Acquisition Board
FBE I & II	- Floodbeam Experiment I & II
FWHM	- Full-Width-Half-Maximum
GUI	- Graphical User Interface
IP	- Inward Path
KAFB	- Kirtland Air Force Base
NMSU	- New Mexico State University
OCS	- Optical Cross Section
OP	- Outward Path
RHINO	- Real-time Histogram Interpretation of Numerical Observations
SOR	- Starfire Optical Range
STTR	- Small Business Technology Transfer

1. Introduction

Laser pointing systems, particularly those used for ground illumination of space objects, are often subject to severe energy limitations when the target has a diffuse Lambertian surface. This is to be contrasted with satellites specific to geodesy, such as LAGEOS, which provide highly enhanced returns using retroreflectors. With even state-of-the-art lasers, the projected beam for Lambertian targets must be very narrow, often on the order of several microradians full-width-half-maximum. Tightly projected beams are subject to pointing disturbances due to atmospheric effects and telescope mechanical vibrations. Knowledge of the magnitude of the disturbances can be very useful; however to obtain a measure of the disturbances extended sensors (target boards) at the object are required. This is impractical for existing space assets.

Beginning in 1997, Nukove developed a technique[1] to assess pointing disturbances based solely on knowledge of the received time-series total signal. The reduction of data from the experiments performed at Starfire Optical Range on Kirtland AFB, NM led to this discovery. Nukove's initial efforts were performed after-the-fact; however the primary lag in obtaining estimates was the preliminary reduction of data from experiments. Because Nukove's techniques do not require imaging or a target board, it was clear that the incoming experimental data could be analyzed on a frame-by-frame basis. This would allow an operator during an experiment to view a screen and make adjustments on the fly or, ideally, provide for automated control to minimize, for example, the static pointing offset known as boresight. Demonstrating the feasibility of such real-time estimates was the fundamental thrust and success of the work performed under the Phase I STTR grant.

2. Background

In 1993, the Surveillance Technologies Branch of the Directed Energy Directorate at the Air Force Research Laboratory, Kirtland AFB, NM (AFRL/KAFB), began a series of three ground-to-space laser illumination experiments at the Starfire Optical Range (SOR) with goal of illuminating low earth orbit satellites and collecting the received focal plane signals. The satellites were at nominal altitudes of 1000km. The efforts were known as Floodbeam Experiment I & II (FBE I & II, 1993 and 1996) and the Active Imaging Testbed (AIT, 1999). Nukove was involved in data analysis after-the-fact.[2,3]

For FBE I & II illumination was at 1.315μm and for AIT the laser wavelength was 0.532μm. The receiver for FBE I was a 1.5m telescope and for FBE II and AIT it was a 3.5m telescope. The lasers were pulsed with low average power; however numerous good returns were collected. The pulse repetition rate during FBE I & II was $1/7^{th}$Hz and resulted in 25-30 illuminations per satellite pass. For AIT the laser was pulsed at 1Hz with bursts at 5Hz and during AIT there were hundreds of engagements, some producing >500 returns for a single satellite pass.

The far-field full-width-half-maximum (FWHM) on FBE I & II was 7μrad and on AIT it was 3.5μrad. These tight beams were dictated by energy requirements and as a result mechanical and atmospheric errors (see Section 5) caused numerous miss-hits. Understanding how well a laser system is pointing therefore is critical in the field.

The low pulse rate during FBE I & II led Nukove to develop a pointing estimation technique for a few as 25 returns. Hypothesis testing with limited data is handled very well by the familiar χ^2 technique. Nukove's approach (see Section 5) differs from the usual hypothesis testing, for example whether a coin is fair, by testing data against ~1,700 predetermined probability distributions for a given scenario (beam size, target approximate dimension...). The best match as determined by the χ^2 confidence Q provides the estimate of pointing.

The determination of the probability distributions is CPU intensive therefore it is performed for specific scenarios and stored in the key χ^2 analysis tool before use. The fact that estimates of system pointing may be obtained with 25 illuminations led to the fundamental effort for Phase I: Determine the feasibility of developing a real-time estimation tool based on Nukove's after-the-fact estimation tool. To this end, Nukove developed RHINO (Real-time Histogram Interpretation of Numerical Observations, Section 6), an Excel® based tool. Both simulated and laboratory data are streamed into RHINO and real-time estimates of pointing characteristics known as *jitter* and *boresight* are calculated and displayed.

3. Objectives, Accomplishments and Proof of Feasibility

This short section simply lays out the objectives of Phase I, the accomplishments and the proof of feasibility.

3.1. Objectives

The primary objective during Phase I was to take the existing Nukove pointing estimation tool and convert it to a graphical-user-interface (GUI) tool and to demonstrate simulated and laboratory generated data streamed into the tool and the determination of real-time estimates of pointing displayed as the data streams in.

The secondary objective during Phase I was the development of a laboratory experiment to emulate laser illumination of objects and the collection of received signals. The objective was a testbed that would allow for experiments to include the potential for a variety of target sizes and pointing conditions.

3.2. Accomplishments

RHINO is the product of the primary objective and will be described in detail in Section 6. It has been blind-tested numerous times. Interesting effects due to target size, etc., have been discovered and biases that are introduced will be a major area of study during Phase II.

The laboratory experiment was successfully developed at New Mexico State University (NMSU) and is described in Section 7. At its simplest, a laser projects a beam with a nearly Gaussian pattern at the target. The beam is steered randomly using a stepper mirror controlled by a commercial package LabView™. The reflected signal is recorded and ready for processing by RHINO.

The Phase I effort produced three conference presentations and associated papers. The first two[4,5] were presented at the SPIE Annual Meeting (Denver, August 2004). The third[6], a compilation of the first two, was presented at the SPIE Europe Conference on Remote Sensing (Gran Canaria, Spain, September 2004) and provided considerable international exposure for the project.

3.3. Proof of Feasibility

The development of RHINO together with the streaming of data and real-time estimation of laser system pointing characteristics has clearly proven the feasibility of developing a tool to be used by laser illumination systems, such as those on SOR and at the AMOS facility on Maui. The addition of the laboratory emulation of a laser illumination system and the collection and successful analysis of the data further establishes the feasibility.

4. Key Personnel

The Phase I Team consisted of two partners with Nukove as prime contractor and the Klipsch School of Electrical and Computer Engineering at NMSU as University partner. The key personnel are described next.

4.1. Nukove Scientific Consulting

Susan Chandler, Senior Scientist and Managing Partner at Nukove served as Principal Investigator during Phase I. Her primary technical functions focused on upgrading the Nukove laser system pointing estimation technique (see Section 5) into a working Graphical User Interface (GUI) that allowed for both Nukove and the investigators at NMSU easy access to analysis. Ms. Chandler performed doctoral work in astrophysics at the University of Texas, Austin, under Dr. John Wheeler. Prior to joining Nukove, she was employed by a small business supporting the Air Force Research Laboratory on Kirtland AFB, NM.

Gordon Lukesh, also a Senior Scientist and Managing Partner at Nukove, received a PhD in pure mathematics from the University of Massachusetts (Amherst) in the area of Lie transformation groups and their actions on Riemannian manifolds. He was employed by Hughes Aircraft in Albuquerque before forming Nukove in 1996. At Hughes, he supported numerous programs at AFRL including the FBE I & II as well as studies that led to the ground to space efforts. He served as Program Manager during Phase I and continued his scientific efforts with an emphasis on the development of numerous validation tests for RHINO (Section 6).

4.2. New Mexico State University

The effort at New Mexico State University (NMSU) was led by Dr. David Voelz, Associate Professor in the Klipsch School of Computer and Electrical Engineering. Prior to his appointment in 2001, Dr. Voelz worked at the Air Force Research Laboratory (Albuquerque, NM) for 15 years on laser illumination, imaging and wave front sensing applications.

Dr. Voelz was assisted in the laboratory by graduate student Ms. Santasri Basu. She received her BS in Electrical Engineering in 2000 from Jadavpur University, Calcutta, India. Her areas of concentration include optical holography, digital signal processing, and expert system development.

5. Strategic Laser Systems and Pointing Estimation - Background

The principal thrust of the Phase I STTR program was to determine the feasibility of obtaining real-time laser system pointing characteristics, primarily for ground-to-space illumination experiments. This section provides an overview of strategic laser experiments, an introduction to two facilities that Nukove has worked with extensively, key system terminology, a review of Nukove's χ^2 estimation procedure and examples of results from simulated data and field experiments performed obtained using RHINO (Section 6).

5.1. Strategic Laser Systems – Overview

Strategic laser illumination systems, such as those at SOR on Kirtland AFB, NM, and at the AMOS facility on Mount Haleakala, Maui, HI, described below (Section 5.1.1) are charged with illuminating space assets (satellites, debris) for a variety of purposes. Illumination includes obtaining return signals for enhanced imaging, polarization measurements, space situational assessment and geodesy.

Geodesy, the measurements of site locations to a high level of confidence, generally uses enhanced targets that are covered with retroreflectors (also known as corner cubes). Corner cubes can enhance the return laser signal by as more than six orders of magnitude. These targets can determine site locations to within 1cm accuracy. An example is LAGEOS (http://msl.jpl.nasa.gov/QuickLooks/lageosQL.html).

Experiments performed at both SOR and AMOS use targets that are not enhanced. These targets are generally modeled as Lambertian (diffuse) objects. To receive sufficient signals at the ground site, the projected laser beam must have a very narrow far-field pattern, on the order of several microradians. Atmospheric effects and mechanical vibrations from the telescope are comparable to the required beam size at the target. Nukove's pointing estimation techniques have been used for experiments both at SOR and AMOS after-the-fact. Real-time estimation, the thrust of the Phase I effort, can provide vital immediate feedback in the field.

5.1.1. Strategic Laser Illumination Facilities

Prior to forming Nukove in 1996, Managing Partner Dr. Gordon Lukesh worked at Hughes Aircraft in Albuquerque, NM. During his tenure at Hughes, Lukesh supported programs that were precursors to ground-to-space illumination experiments performed at Starfire Optical Range on Kirtland AFB. SOR has numerous optical telescopes, including a 1.5m telescope used during FBE I and a 3.5m telescope used during FBE II and AIT. Lukesh's principle contact was Dr. David Voelz, then at the Surveillance Technologies Branch at AFRL. Dr.

Voelz is now at NMSU and a partner under Phase I. Nukove has supported data reduction from FBE I & II and AIT as well as other AFRL experiments.

Details about SOR may be found at http://www.de.afrl.af.mil/SOR/.

More recently, through funding by AFRL, Nukove has been involved with experiments at AMOS on Maui. The facility has more than a dozen optical telescopes at 10,000ft, including a 3.67m diameter telescope used for major operations. AMOS is ideally located for the observations of launches out of the neighboring island of Kauai as well as launches from Vandenberg towards Kwajelein Atoll.

Details about AMOS may be found at http://www.maui.afmc.af.mil/.

5.1.2. Pointing Terminology

Three key terms are used to describe laser system pointing characteristics. For a circular transmitter aperture with no aberrations such as atmospheric effects, the beam far-field pattern is well approximated by a Gaussian intensity pattern. Theoretically it is the Fourier Transform of the aperture[7] and involves the circular Bessel function J_1. In practice, and because it is the central portion of the beam that provides the highest intensity, the far-field pattern is usually approximated by a Gaussian, an example of which is shown in Figure 1.

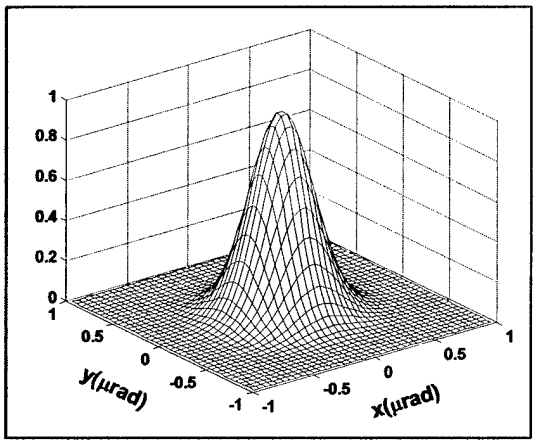

Figure 1. This figure shows a typical Gaussian far-field pattern used for analysis.

Because the Gaussian is the standard approximation for the far-field pattern, it is generally defined by its full-width-half-maximum (FWHM). This is the angular width at which the intensity drops to one-half the maximum.

During FBE I & II[2] wave optics analysis was used to determine that the FWHM of the 1.315μm laser was on the order of 7μrad. During AIT, with the laser operating at 0.532μm, the FWHM was estimated to be 3.5μrad.

The shape of the far-field pattern can be corrupted by atmospheric conditions generally characterized by the Fried coherence length r_0. While it is beyond the scope of this report, it can be shown that when the laser transmitter size lies in the range $1 < D_T/r_0 < 4$, the shape of the central lobe is maintained, including the FWHM. Nukove's estimation tools work well in this regime.

To place such angular units in perspective, a United States quarter subtends approximately 3.5μrad at a distance of three miles. For far-field patterns such as those during AIT, errors in pointing can be substantial. Two terms are used to describe the errors, *jitter* and *boresight*.

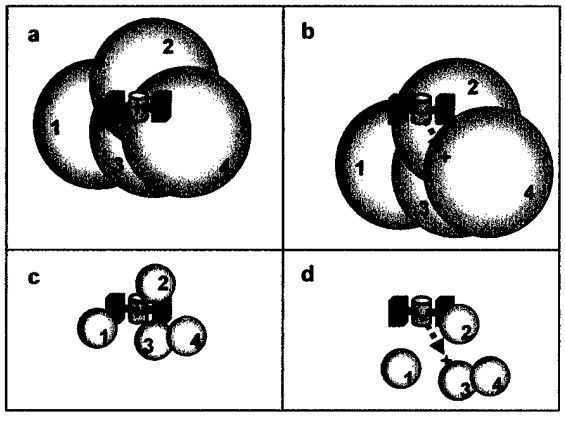

Figure 2. The four figures shows both the effects of jitter and jitter combined with boresight. a) and c) show four successive illuminations in the presence of only jitter, while b) and d) shows the same jitter but with a fixed offset (boresight) as indicated by the arrow. Beam size is critical with pointing errors.

Jitter is the term used to describe the shot-to-shot variation of pointing caused by effects such as atmospheric turbulence and telescope mechanical vibration. Jitter is normally considered to be a two-axis uncorrelated effect, modeled as a zero mean Gaussian disturbance with a 1-σ one-axis standard deviation. Under certain circumstances the along-track and cross-track specifications may differ slightly due to atmospheric effects.

Boresight is the term reserved for a residual optical misalignment. For experiments the boresight is typically budgeted for the experimenters and the system is aligned within the tolerance.

Jitter and boresight may be best understood with a graphic as seen in Figure 2. Four successive shots (1,...4) are shown illuminating a simulated object. In a) there is no boresight offset; simply the effect of the 1-σ two-axis uncorrelated jitter. In b) boresight is added as indicated by the arrow (the same jitter occurrences are used for clarity. It is evident that the relative size of pointing disturbances and the beam FWHM that is crucial: c) and d) show the same disturbances but with a smaller beam.

5.1.3. The Range Equation

Prior to the FBE I & II and AIT field experiments at SOR, extensive studies were undertaken to assess laser energy requirements for various conditions (such as telescope sizes, atmosphere, and expected target cross section). Key to this analysis was the Range Equation. At it simplest, the range equation for received energy is

$$E_{rcvd} = OP \cdot OCS \cdot IP \tag{1}$$

OP is the outward path and estimates the laser intensity at the target. *OCS* is an estimate of the target optical cross section and *IP* is the inward path from the target to the receiver. Figure 3 shows the fundamental elements of a ground-to-space illumination experiment. The three central equations are described next.

The Outward Path
The outward path *OP* determines the laser intensity at the target and is given by

$$OP = \frac{D_T^2 \cdot E_{pulse}}{\lambda^2 \cdot R^2} \cdot trans\_losses \cdot \tau_{atm} \tag{2}$$

In this equation, D_T is the transmitter diameter, E_{pulse} is the laser energy, λ is the wavelength and R is the range to the target. *trans_losses* includes optics transmission, wavefront errors and laser beam quality and τ_{atm} is the atmospheric transmission.

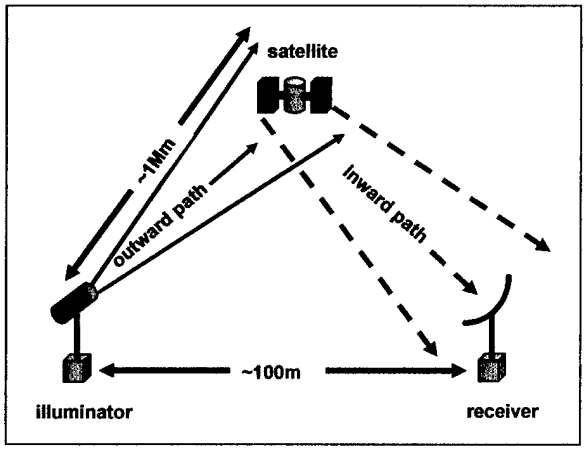

Figure 3. This figure shows the basic elements of a ground-to-space illumination experiment. The illuminator projects the laser at the target for the outward path. Energy is reflected off the target and collected by a receiver. The distances shown are typical for experiments performed both at SOR and Maui.

Optical Cross Section
OCS is a measure of the apparent brightness of the target. A starting point for pre-experiment estimation for targets without retroreflectors assumes that the object is a Lambertian (diffuse) reflector. Equation (3) provides the estimate.

$$OCS = \frac{\rho \cdot A}{\pi} \quad \left(m^2 / SR\right) \tag{3}$$

In this equation ρ is the estimated target reflectivity (albedo) and A is the projected area.

The Inward Path
The inward path *IP*, given by Equation (4) estimates the received energy reflected from the target.

$$IP = \frac{A_{rcvr}}{R^2} \cdot rcvr\_losses \cdot \tau_{atm} \tag{4}$$

A_{rcvr} is the receiver collecting area and *rcvr_losses* includes the optics transmission and detector effects.

In practice, the least well understood term in the Range Equation is *OCS*. For estimates prior to FBE I & II and AIT, the reflectivity was estimated at 0.2 and target size was based on best information about the object. Reduction of data performed by Nukove[2,3] determined that the received signals were well estimated by the Range Equation, often within a factor of two either side of the prediction.

5.1.4. Example of Field Data

The combination of the outward and inward path elements of the range equation produce an R^4 range dependency. As an example, data from satellite 18123 illuminated during AIT is shown in Figure 4.

The figure shows the range to target through the satellite pass in the dark line. The dots represent the received energy in photons. The received energy lies under an umbrella that demonstrates the range dependency very clearly.

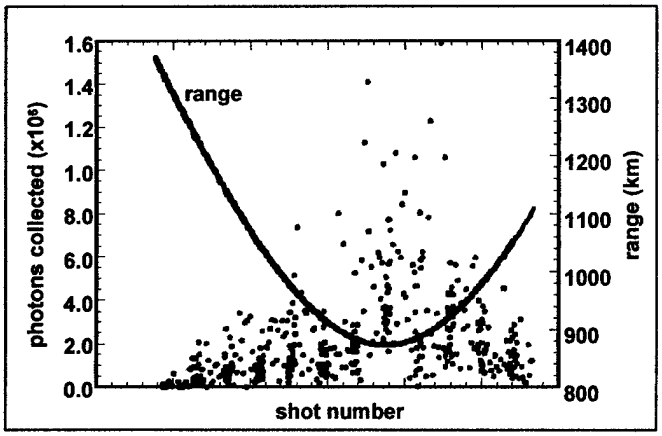

Figure 4. This figure shows the effect of range (R^4) for the illumination of satellite 18123 1 Nov 1999 during the AIT experiment. The black line shows the range and the dots shows the received signal, under an R^4 envelope.

What is important to note about the received energy is the fluctuations from shot to shot. This is due to the pointing jitter in the system (Section 5.1.2) that causes the beam to miss the target frequently. Beginning in 1997, Nukove developed a technique to take the shot to shot received signal and, accounting for such things as range variations and variations in atmospheric transmission due to elevation changes, estimate the magnitude of the pointing jitter (and boresight).

The approach[1], reviewed next, is χ^2-based and can provide pointing estimates with as few as 25 returns. The principal thrust of this Phase I effort was to take the Nukove technique, used after-the-fact for analysis of FBE I & II and AIT and determine the feasibility of developing a real-time field estimation tool. A review of the Nukove technique is warranted.

5.2. Limited Data Pointing Estimation Technique - Review

During FBE I & II the laser repetition rate was 1/7thHz. During a typical satellite pass there were 25-30 illuminations after the satellite rose above 45° elevation, passed over SOR and dropped to 45° elevation. Safety concerns limited illumination to above 45° elevation. Nukove recognized that such limited data sets are best handled via the familiar χ^2 test.

Nukove advanced the χ^2 test to handle multiple hypotheses simultaneously. Consider the following simple example of a coin toss, the standard first example of the test. Typically the test of fairness is whether a tossed coin results in an expected frequency of 50% heads and 50% tails. However, there is no reason a coin could not be tested against multiple hypotheses, such as heads-tails 0%-100%, 10%-90%...100%-0%. The χ^2 statistical confidence Q with the highest value would provide a test of the coin.

For pointing estimation, that is the determination of jitter and boresight (Section 5.1.2), Nukove developed ~1,700 hypotheses for the testing of pointing for specific scenarios (beam FWHM and target extent). The simulations provided the signal returns from 100,000 illuminations of a target. Each 100,000 illuminations were for a specific simulated input jitter and boresight (ranging from 0xFWHM to ~1.2xFWHM). Each simulation resulted in a histogram of returns. Figure 5 shows an example for j = 0.3xFWHM and b = 0.2xFWHM. This represents exceptional pointing, yet the target is not always fully illuminated.

The histogram must be interpreted as follows: Unity on the x-axis represents the counts from perfect target illuminations while zero represents the number of total miss-hits. The histogram may also be considered a probability distribution function for the jitter / boresight input.

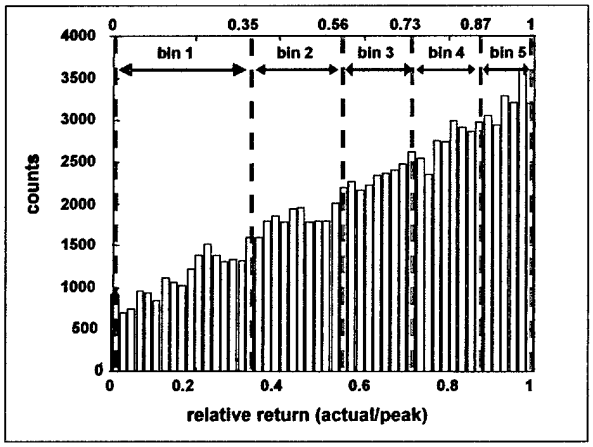

Figure 5. This histogram shows the counts from 100,000 simulated returns with the pointing hypothesis j=0.3xFWHM and b=0.2xFWHM. Counts at unity on the x-axis represent perfect pointing and those at zero indicate a complete miss-hit. The counts are divided equally into five bins of 20,000 returns and the bins supply the necessary tool for testing the hypothesis that a finite data set arises from the input pointing.

For the use of χ^2 testing, the bins, or more properly the bin endpoint pairs, allow for the testing of a finite set of data against ~1,700 hypotheses for pointing that range from 0 to 1.2xFWHM in both jitter and boresight. The approach is quite straightforward. For a finite set of data, such as 25 shots, with proper normalization count the number of occurrences in each of the five bins for each of the ~1,700 bin-pair. If the data arose from a specific jitter / boresight pair, the expected frequencies per bin would be all fives. χ^2 would equal zero and the associated confidence Q would equal 100%

The bin-endpoint pairs play the same role as allowing for the counts in frequency from the toss of a coin. The fact that 25 data points can provide good estimates of pointing allowed for the development of RHINO, discussed next. The key point is that while the determination of the histogram bin-endpoints is CPU intensive it is performed in advance. Actual testing of 25 data points in nearly instantaneous.

5.3. The Validity of χ^2 Testing of Pointing Hypotheses

The application of a χ^2 test to limited data sets requires that the data follow "reasonable statistics" such as Gaussian or Poisson[8]. For example, a fair coin tossed ten times has an expected frequency of occurrences of heads and tails both five. When tested repeatedly, the occurrences are seen to be normal distributions of heads and tails each with mean five.

To test the applicability of χ^2 testing of pointing hypotheses using the binning method (Section 5.2), a single example was chosen. The case assumed a beam FWHM = 3.5μrad, with jitter = 2.5μrad and boresight = 2.0μrad. The test was to determine the frequency of occurrences within each of the five bins, thus 10,000 realizations of 25 shots were simulated have the same pointing errors, and the counts per bin were recorded. The expected frequency per bin was five. Figure 6 shows the distribution within each bin as distinctly Poisson, thus the χ^2 approach appears applicable. During Phase II a sophisticated statistical study will be used to show that the Poisson distributions exist for each pointing estimation bin set.

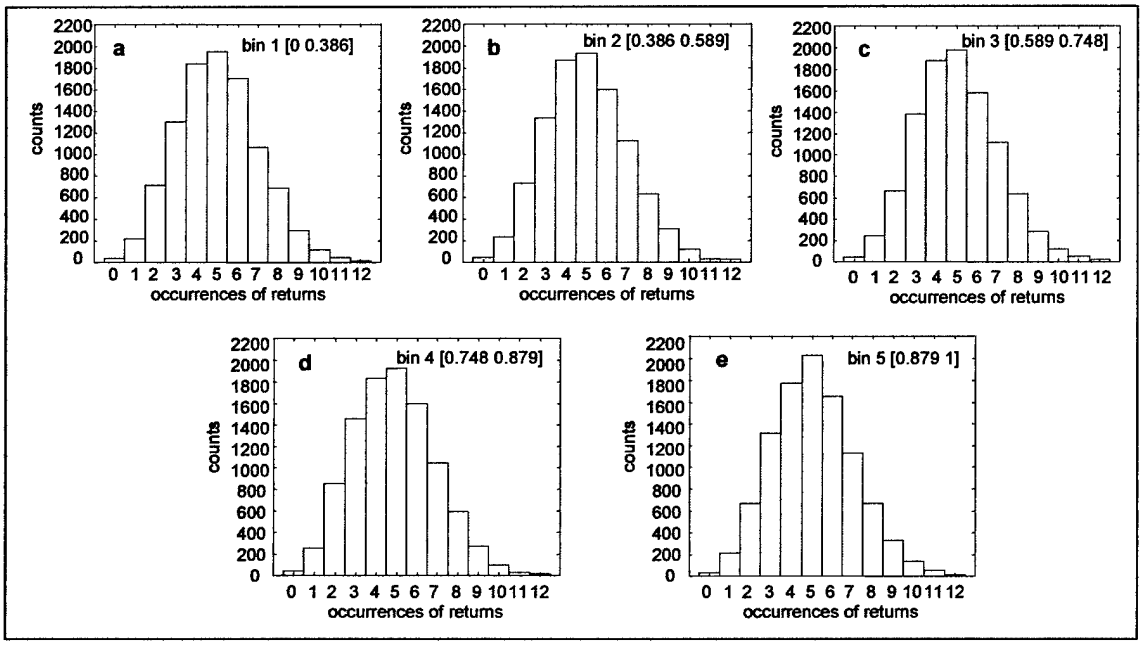

Figure 6. This figure shows the frequency distribution of counts for one specific example of pointing estimation. 10,000 realizations of 25 shots were simulated and the counts per bin retained. The 10,000 realizations had the same pointing characteristics as the bin sets and the distributions are clearly Poisson suggesting the χ^2 approach is valid.

6. RHINO (Real-time Histogram Interpretation of Numerical Observations)

Nukove's prime effort during Phase I was the conversion of its existing after-the-fact pointing estimation approach into a real-time estimation tool. To this end, Nukove developed RHINO (Real-time Histogram Interpretation of Numerical Observations) and clearly, through streaming data, established the feasibility to produce a real-time tool for both laboratory and field use. This section describes the basic steps taken, the key elements of RHINO, examples of simulated data analysis and examples from field data.

Prior to the development of RHINO, estimates of pointing for limited data sets were obtained manually. Data was pasted into an Excel® spreadsheet and the estimates were displayed. The tool was static, however many of the elements necessary to convert the tool into a dynamic, real-time product for estimation were available. Section 6.1 discusses the major steps taken. Sections 6.2 and 6.3 show examples of simulated and field data.

6.1. RHINO Development

There were five main areas in the development of RHINO. First and foremost was obtaining the ability to have running estimates (Section 6.1.1). This was followed by graphics enhancement (Section 6.1.2), a link to Matlab® for bin development (Section 6.1.3), creation of an Excel®-based GUI (Section 6.1.4) and the addition of a video recording capability (Section 6.1.5).

6.1.1. Running Estimates

The main thrust of Phase I was to establish the feasibility to take streaming data and provide running estimates of pointing conditions. This led to enhancement of the existing spreadsheet to allow for large data sets, with data streamed in as follows: Data points 1-25 are normalized and an immediate estimate of jitter and boresight is made. Then data points 2-26, 3-37... are similarly analyzed. Thus each running set of 25 data points (simulating data obtained in real time in the field) provides an estimate. The current status of RHINO is that a large data set is

created and drawn from after-the-fact, however the streaming nature of the input proves the feasibility of RHINO as a field tool.

Nukove also included a 200 point moving average of the estimates. Thus after 225 points have been analyzed a smoothed estimate is available. As shown in Section 6.2, the 200 point moving average provides excellent estimates of pointing for simulated data.

6.1.2. Graphics Enhancement

There are two primary uses for RHINO in the field. The first is to provide real-time pointing information for an operator in a visual manner. Thus as the data estimates, both from 25 points and from the moving average become available, they are displayed in real time on a RHINO screen. An example is shown in Figure 7. In practice the

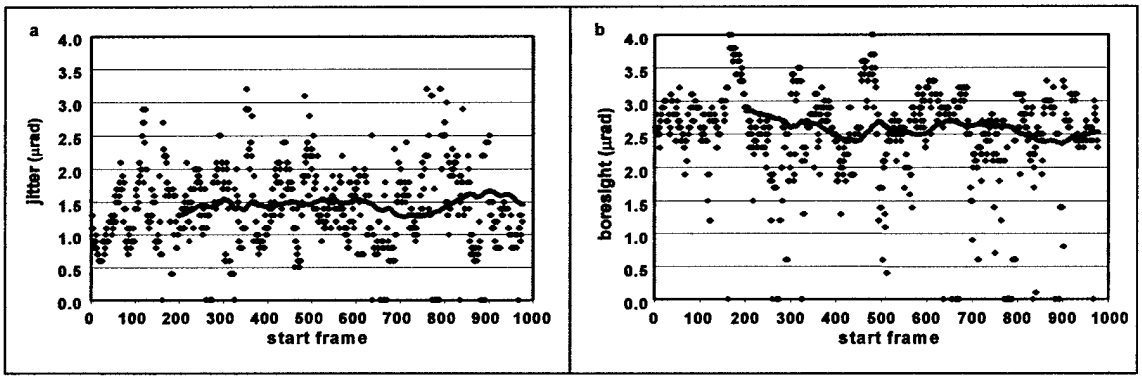

Figure 7. This figure shows the display an operator will see while data is streamed into RHINO. In practice as the data is streamed in both displays (jitter on the left, boresight on the right) are dynamic. The first estimates after 25 points appear as the dots. After 200 estimates the running average is dynamically displayed.

data display is dynamic: As field data is streamed into RHINO estimates of jitter (a) and boresight (b) are displayed as dots appearing from left to right after the first 25 data points have been analyzed. After a total of 225 points have been streamed in the 200 point running average is dynamically displayed. Thus an operator can view the system performance in real time and make adjustments, for example to correct the boresight error, on the fly (see Section 6.2).

6.1.3. Link to Matlab®

The generation of bin models is performed in Matlab® and is time consuming. RHINO has a link to Matlab to allow for an operator to generate a new set of bin models when needed. Currently this requires the operator to have Matlab but under Phase II, Nukove will use dynamic link language (.dll) and obtain a compiler for Matlab so that the entire package will be self-contained. The introduction of the link in the current form of RHINO is the first step towards the self-contained package.

6.1.4. Excel® GUI Format

To use RHINO, the operator has several options as shown in Figure 8 and described next.

Object: For each, the user selects an object type. Current objects include reflectivity maps of space satellites illuminated during AIT as well as a cornercube (a directional reflector) and simple shapes such as circles and bars.

Boresight angle: Several models Nukove has developed include the ability to put in a boresight offset and choose a fixed boresight angle. Nukove has shown[9] that by steering in boresight offset and around an object it is possible to distinguish simple shapes without imaging.

Atmosphere: The user may specify D/r_0, the ratio of the transmitter aperture to the Fried coherence length r_0. For values of this ratio of 1–4, the central lobe of the far-field pattern is well preserved. As D/r_0 approaches 4, energy

is distributed to the wings of the pattern and causes a fluctuation in the on-axis intensity. When D/r_0 is greater than 4, the beam is too broken up to be useful.

Beam size: While many models are in units of μrads at the target, any units may be used. Laboratory models may also be imported. For example, when working with NMSU data the beam FWHM is given is mirror stepper units and the outputs (see Section 7) are tailored appropriately.

Beam type: The final choice shown is the beam type. Currently RHINO has several options including diffraction limited, a simulated beam projected from the Air Force Maui Optical Site (AMOS) facility on Mt. Haleakala (Maui, HI), typical beams used during AIT, and the measured NMSU laboratory beam. The beams in space were generated with wave-optics propagation codes.

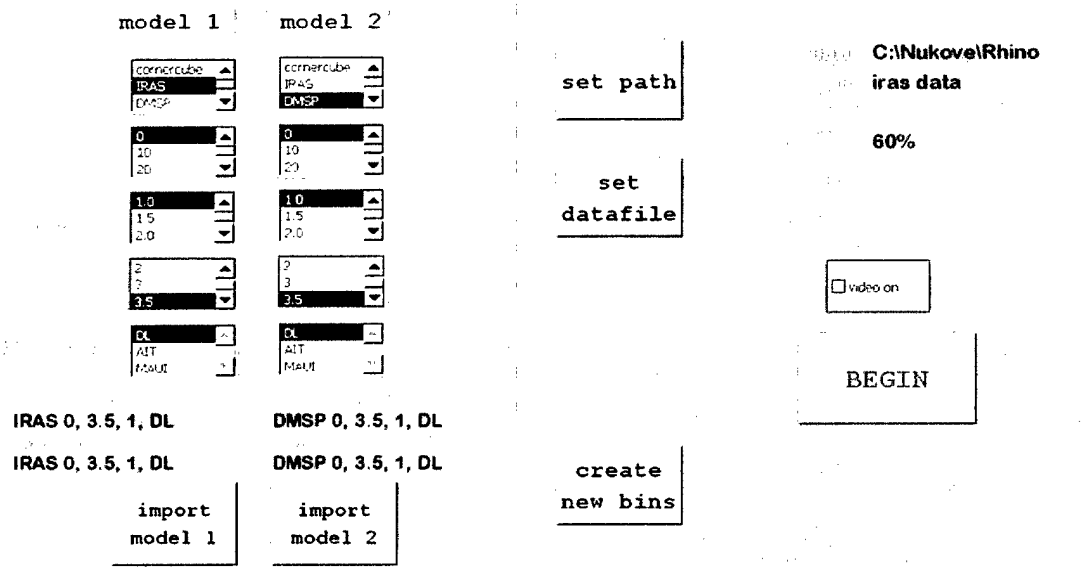

Figure 8. This is the current GUI of RHINO. Numerous choices are available to the user, such as the object type, beam size, and beam type. When the user hits "import model 1" or "import model 2" the package will either import existing models or prompt the user "create new model". Some of the parameters to set are the cutoff Q and the number of points for the moving average. A video may be made of the output.

The next step is to import the model. Two events can happen. Either the model exists and is imported or it needs to be created. Should it need to be created (currently ~20 min) RHINO calls Matlab® automatically and does the work. Because this is time intensive it should be done well in advance of an engagement. After a path to the data file is put in, the data set may be processed through RHINO. RHINO automatically creates graphics, examples of which are the subject of Section 6.2. The Appendix shows RHINO graphics available to the user.

6.1.5. Video Recording

An additional option is to create a video using a screen recorder package from TechSmith called Camtasia Studio™. By clicking the option, the code generates a frame-by-frame video for storage and playback. The current version of Camtasia must access DOS for a frame-by-frame recording and is slow. For real-time estimation with a high repetition laser a 15 frame/sec recording can be made.

6.2. Examples from Simulated Data – Validation Tests

Nukove has performed extensive validation tests of RHINO. These have been done blind, i.e., with data created by one person and given to another without knowledge of the input pointing parameters. RHINO performs extremely well, producing a prediction for nearly every frame of data. The test cases point out a tendency for a bias in the estimates, particularly with an extended target. Nukove will continue to investigate these biases with the ultimate goal to quantify them for eventual removal. Three examples are shown in this section. Two jitter and boresight estimates, and a boresight estimate showing a correction half way through. The boresight correction example is fundamental: With a high repetition rate system, when a boresight error is identified the laser pointing may be steered in an attempt to correct the error. The angular direction of the boresight error is unknown so a con-scan or gradient search may be necessary.

In the four examples the units are μrad and the beam FWHM = 3.5μrad, typical of the beam size during AIT. The target is a circle with diameter 1.5μrad. The cutoff Q, i.e., the minimum confidence for an estimate to be accepted was set at 60%.

6.2.1. Example 1: j = 1.0μrad, b = 3.0μrad

This first example is RHINO output of the pointing estimates for simulated collected data with pointing errors of j=1.0μrad, b=3.0μrad. Successive sets of 25 data points are used to get each value of the predicted jitter. Figure 9 shows the estimate with jitter a) and boresight b) .Points 1–25 are represented by the dot at start frame=1, etc. The points at 0 reflect that the Q for the frame was less than the cutoff Q of 60% and the estimate was not accepted. The black line indicates the 200 point moving average. (The zeroes from the unaccepted estimates are not included in this quantity.) The jitter estimate from the 200 point moving average is slightly too high at 1.5μrad and the boresight estimate is slightly too low at 2.5μrad. This 0.5μrad difference may be due to the choice of j and b when the peak Q is multivalued, or a bias due to the finite size of the object, or perhaps even to a limit on the accuracy with which these quantities can be determined.

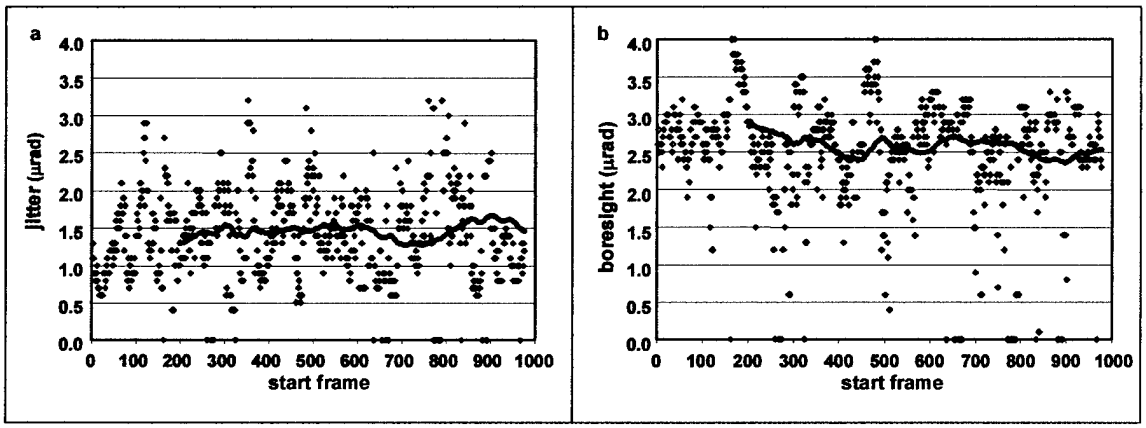

Figure 9. This figure shows the frame by frame estimates for simulated data from returns with j=1.0μrad and b=3.0μrad. (a) shows the jitter estimate and (b) shows the boresight estimate. The dots are the frame by frame estimates and the solid line is the 200 point moving average. The points with both jitter and boresight at 0 reflect that the Q for the frame was less than the cutoff Q of 60% and the estimate was not accepted.

6.2.2. Example 2: j = 3.0μrad, b = 2.0μrad

For this example the jitter is increased to 3.0μrad and the boresight is reduced to 2.0μrad compared to the previous. Again, the points at 0 reflect that the Q for the frame was less than the cutoff Q of 60% and the estimate was not accepted. The 200 point moving average from RHINO (unaccepted zeroes not included) gives a jitter estimate of 2.5–3.0μrad and a boresight estimate of 2.5–3.3μrad, as shown in Figure 10. As in Example 1, the RHINO estimates are slightly off. This 0.5μrad difference may be due to the choice of j and b when the peak Q is multival-

ued. Currently when multiple estimates are returned, RHINO chooses the jitter/boresight estimate using the peak Q with the lowest jitter and the highest boresight. This approach is the subject of on-going investigation.

A simple speculation may indicate why biases are present. Consider the extreme of a target that is infinite in extent and uniform in reflectance. When a laser with pointing jitter illuminates the target, the returns will be constant and any estimation tool will return a jitter value of zero. Targets that range in size between a cornercube and infinite extent must exhibit biases dependent of their size.

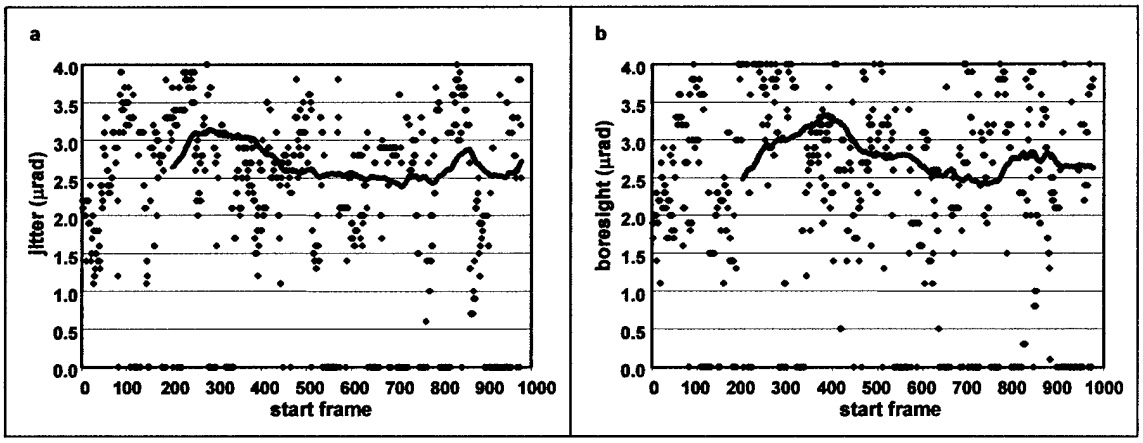

Figure 10 . This figure shows the frame by frame estimates for simulated data from returns with j=3.0μrad and b=2.0 μrad. (a) shows the jitter estimate and (b) shows the boresight estimate. The dots are the frame by frame estimates and the solid line is the 200 point moving average. The points with both jitter and boresight at 0 reflect that the Q for the frame was less than the cutoff Q of 60% and the estimate was not accepted.

As part of on-going efforts, the biases evident in Figure 9 and Figure 10 will be quantified using RHINO for a range of target, beam, and pointing errors. When quantified, the biases will be accounted for automatically in RHINO.

6.2.3. Example 3: Reduction in Boresight

This final example of pointing estimates shows one of the main goals of RHINO, i.e., that we can monitor changes in the pointing parameters. Armed with a boresight estimate and using an intelligent search (con-scan, gradient) the boresight may be corrected either by an operator or using feedback. Figure 11 shows the boresight estimate with 2,000 simulated shots. For the initial 1,000 shots the boresight was 3.0μrad and was then reduced to 2.0μrad. RHINO clearly computes this reduction, which is evident shortly after shot 1,000. As in previous examples, the 200 point running average under predicts the boresight by 0.5μrad. Determining the direction of the boresight correction by 1.0μrad is beyond the scope of the current effort. In a field experiment, such a reduction would lead to more shots with higher returns and more success for an experiment. (The points at 0 reflect that the Q for the frame was less than the cutoff Q of 60% and the estimate was not accepted. These points also are not included in the running average.)

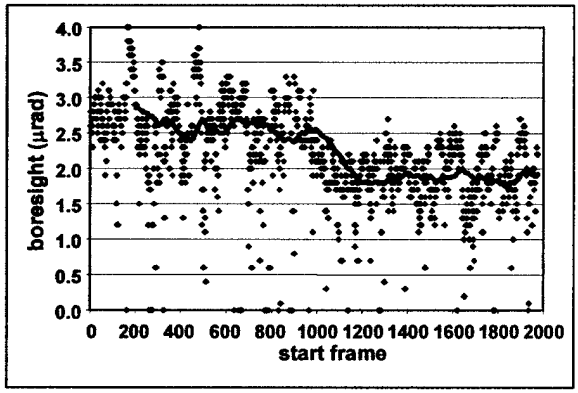

Figure 11. This output from RHINO shows a reduction of boresight by about 1μrad starting at shot 1,000. The points at 0 reflect that the Q for the frame was less than the cutoff Q of 60% and the estimate was not accepted.

6.3. Examples of Estimation from Field Experiments

Through its collaboration with the Surveillance Technologies Branch at AFRL, Kirtland AFB, Nukove has participated in considerable data reduction from ground-to-space illumination experiments. The majority of the efforts was directed analysis of data from FBE I & II[2] and AIT[3]. More recently Nukove has been involved with experiments carried out at the AMOS facility on Mt. Haleakala, Maui, HI. While the experiments have objectives beyond the scope of this report, Nukove was able to use RHINO to establish that there were difficulties with the system pointing. Nukove analyzed data taken in August 2003 for illuminations of the Explorer satellites. One example is shown in Figure 12. The target in this case was Explorer27 on 22 August 2003.

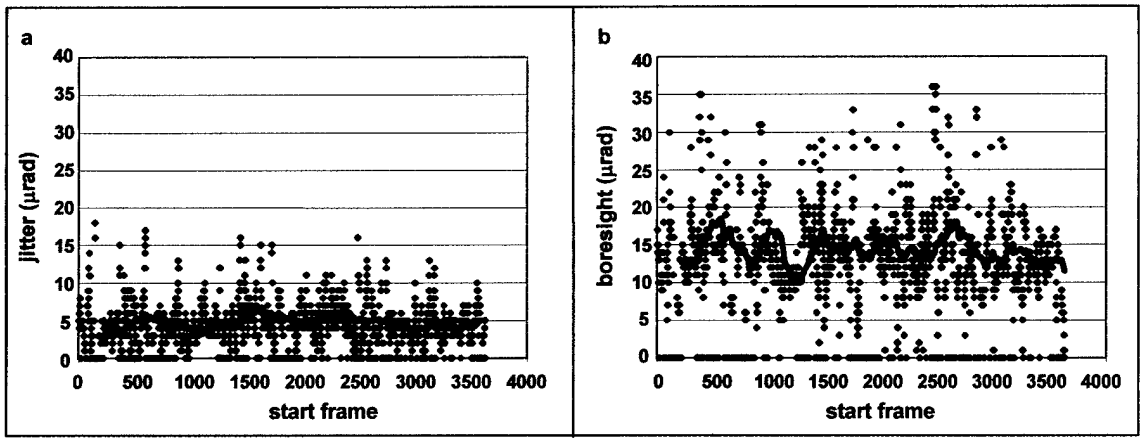

Figure 12. This figure shows analysis of pointing from an experiment at the AMOS Facility, Maui. The target was Explorer27 on August 22, 2003. The large jitter estimate (nominally 5μrad) and boresight greater than 10μrad pointed towards system problems requiring attention by the experimenters.

The large jitter estimate was troubling for the experimenters, whose budget is considerable smaller. The wild fluctuations in boresight are due to two facts. First, the illumination used a human-in-the-loop to provide time-of-flight lead ahead as opposed to FBE I & II and AIT which both had automated lead ahead. Second, the beam was often steered away from the target deliberately to allow for measurements of the sky background.

This data was analyzed several months after the fact. The utility of real-time estimates is very clear: The human-in-the-loop can monitor critical pointing parameters, especially boresight, and intervene to force better pointing. There is also the potential for automated control, a subject of the Phase II efforts. Boresight estimates will be fed back and used to make alterations in pointing using, for example, a conical scan.

To provide an intermediary between simulations and field experiments, Phase I included the development of a laboratory experiment at NMSU. As described next, the experiment emulates the ground-to-space illumination experiments and does so in a repeatable manner to allow for analysis of pointing estimation under a variety of conditions. During Phase II, NMSU will include such elements as phase screens to introduce atmospheric turbulence.

7. Laboratory Experiment

Two versions of the testbed were developed during Phase I. Initial tests were performed using a direct illumination approach, whereby the detector served as the receiver. In the second version, which more accurately emulates a ground-to-space experiment, a reflective target was introduced as well as a collecting aperture.

7.1. Direct Illumination Layout

The setup in the first version was simplified with the detector being illuminated directly by the laser beam. This ensures sufficient energy for measurements. A 1.5 mW HeNe laser beam is input to a 10X beam expander and the output beam, which has a FWHM of about 0.64 cm, reflects off a steering mirror and illuminates a photodiode detector. The detector is considered a point receiver, as its area is small ($1mm^2$). The setup is shown in Figure 13.

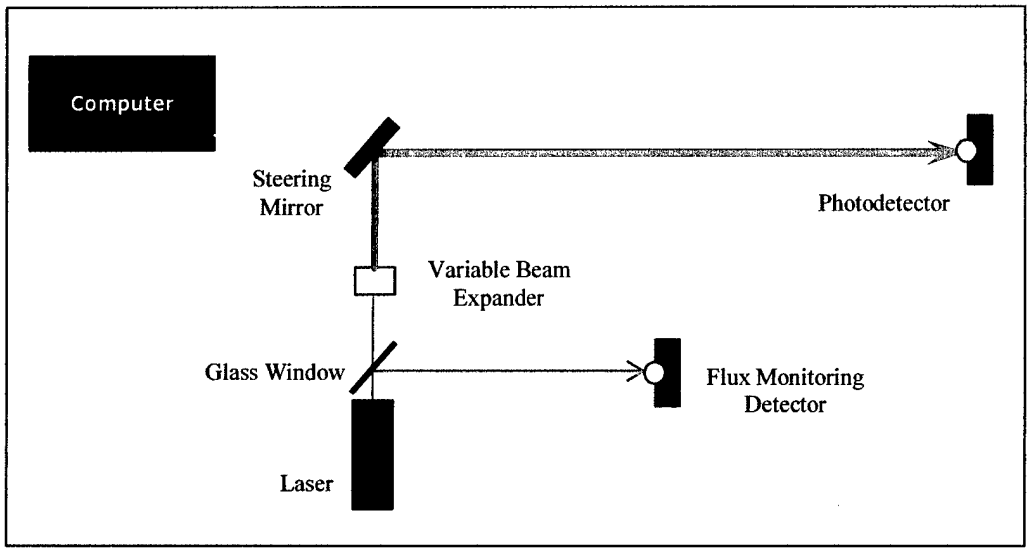

Figure 13. This figure shows the direct illumination experimental set-up. The HeNe laser is directed at the detector. The variable beam expander allows for choices of beam size and the glass window splits off a portion of the laser energy to monitor fluctuations. The steering mirror, controlled by a commercial package LabVIEW introduces controlled disturbances.

The set-up is useful for testing in the laboratory without the complications of a reflective target. A small percentage of the initial laser beam is picked off with a glass window and directed to a second photodetector. The signal on this detector is used to monitor flux changes in the laser. The signals from both detectors are digitized and recorded in the computer through a digital acquisition board (DAQ) board.

Beam jitter and boresight errors are simulated by moving the steering mirror, which is driven by computer-controlled actuators. A LabVIEW program was written to control the actuators and record the photodetector signals after a mirror movement. Gaussian random number generators (for both x and y angular coordinates) create values that are sent to the mirror in order to simulate beam jitter. A constant angular offset can be sent to the mirror to simulate beam boresight error. The program generates the x- and y-angle inputs for the steering mirror every 8 seconds where the delay is necessary to insure all movement has stopped before the photodetector readings are captured. The data recorded in the computer is formatted as an Excel spreadsheet file and sent to the window under which RHINO is operating. Increasing the data rate from the testbed will be investigated during Phase II.

7.2. Reflective Target Layout

A reflective target is used in the second version. The system setup is as shown in Figure 14. The experimental setup employs a target made of reflective tape fixed to glass and placed in the illumination beam. For the results presented in this paper we used a square target that was very small compared to the beam FWHM, so it was assumed to act as a point target. The light reflected from the target was low in intensity so a 5cm diameter lens was placed in front of the detector to collect more light as well as reduce speckle effects.

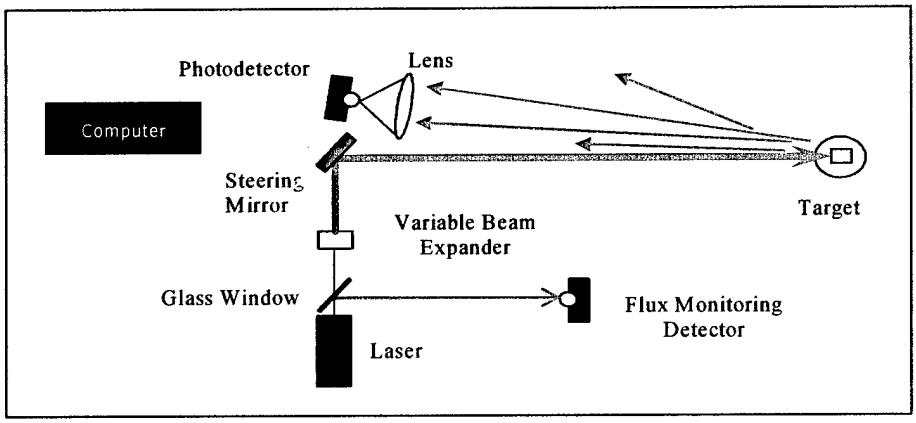

Figure 14. This experimental set-up more accurately emulates a ground-to-space illumination experiment by introducing a reflective target and collecting lens. The other elements in the layout remain the same as in Figure 13.

7.3. Experimental Results

As discussed in Section 5.1.2, the relative size of pointing errors and the beam FWHM is the critical comparison. For the NMSU set-up, the beam pattern, shown in Figure 15, had a FWHM = 0.2SU (where SU is units of mirror motion, known as stepper units). The beam is largely a Gaussian and sufficient for the experimental efforts. A variety of disturbances in stepper units were introduced using LabVIEW, the data was collected and analyzed by RHINO.

Results were very good and also pointed to a distinct bias in the estimation process that has been noted through simulations. A major area of research during Phase II will be to understand from a fundamental statistical point of view, why such biases exist. Provided the biases are quantifiable and repeatable they pose no fundamental difficulties as they may be accounted for in RHINO software.

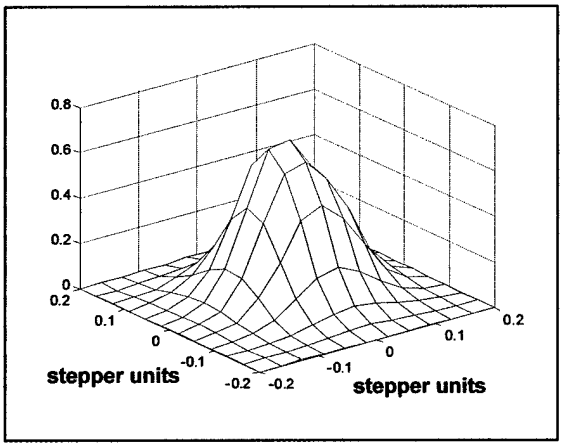

Figure 15. This figure shows the measured NMSU beam at the target. The FWHM is 0.2SU where SU are stepper units for the mirror that introduces disturbances.

An example of results from the laboratory experiment is shown in Figure 16. In this example the jitter 1-σ specification was 0.057SU and the boresight was 0.114SU. The RHINO estimates are very good.

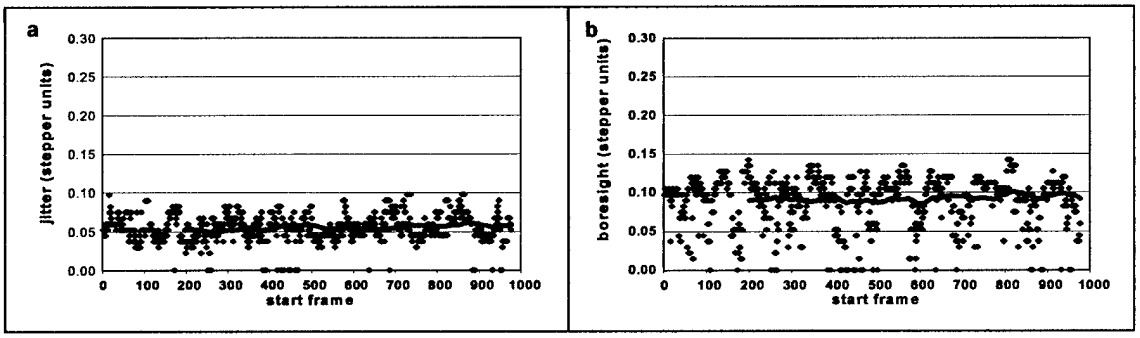

Figure 16. Testbed example with (a) jitter and (b) boresight estimation for j = 0.057 SU, b = 0.114 SU. The 200-point moving average shows an average jitter estimate (~0.05) that is very close to the input value and an average boresight estimate (~0.095) that is slightly lower than the input value.

8. Future Efforts

The work performed under Phase I was extremely successful at establishing the feasibility of obtaining real-time field estimates of laser system pointing. It also served another purpose by defining key elements of work that need to be performed during Phase II. These include, but are by no means limited to:

- Develop an understanding of the biases introduced by the relative size of the beam and target, through simulations, detailed statistical analysis and laboratory experiments
- Establish through statistical analysis the Poisson distribution shown for one specific bin model (Section 5.3) is true for all
- Establish through detailed statistical analysis as well as simulations whether the use of adaptive bin sizes will provide more robust estimates of pointing estimations
- Upgrade the laboratory testbed to include phase screens to introduce repeatable atmospheric turbulence and through the use of clever optics, different levels of turbulence
- Increase the data collection rate capability of the testbed and perform the final link between the testbed and RHINO
- Develop schemes for adaptive reduction of boresight errors (Figure 11) with a goal of automating the procedure

Funding under the Phase II grant will allow for successful investigation of the key issues identified.

9. Conclusions

The Phase I effort has been a success. The fundamental goal was to establish the feasibility of obtaining real-time estimation of laser system pointing. As shown in the Final Report, the feasibility was proven via the development of RHINO and the testbed at NMSU and the demonstration of streamed data with real-time outputs displayed for an operator. RHINO is currently used to provide after-the-fact estimates of pointing for on-going experiments at AMOS through funding by AFRL.

As detailed above (Section 8) numerous enhancements and areas of study were identified. The Phase II funding will allow for eventual field use of RHINO; a key goal of this STTR.

The efforts during Phase I also produced three technical papers and presentations[4,5,6] that provided much needed visibility for the Phase I efforts and feedback as the team prepares for Phase II. The first two papers were presented at the Annual Meeting of SPIE (Denver, 2004) and the third was presented at SPIE Europe, Gran Canaria, Spain, September, 2004).

10. Acknowledgements

Nukove would like to thank Dr. Jon A. Sjogren of AFOSR for his support for this work under a Phase I STTR Grant #F24920-03-C-0064. Nukove is also pleased to acknowledge to efforts of NMSU developing the operational testbed. The Nukove/NMSU Team looks forward to continued work during Phase II.

Appendix A. Examples of RHINO Graphical Capabilities

This Appendix shows five typical windows available from the Phase I RHINO GUI. Operators may choose to display one or more of these windows simultaneously, for example jitter and boresight may be selected.

Example 1. Jitter Dynamic Display with 50 Point Moving Average

Figure 17 shows analysis of pointing jitter from the illumination of Satellite 2102 during AIT. In this example a 50 point moving average is displayed. As the operator would see the display, the first data displayed will be a point at x-axis index 1 representing an estimate from the first 25 shots. After 50 such estimates the moving average is displayed as a black line. The display is dynamic when RHINO is employed. The black box displaying 1.10 is the final 25 shot pointing estimate, however when the display is dynamic the number is constantly updated.

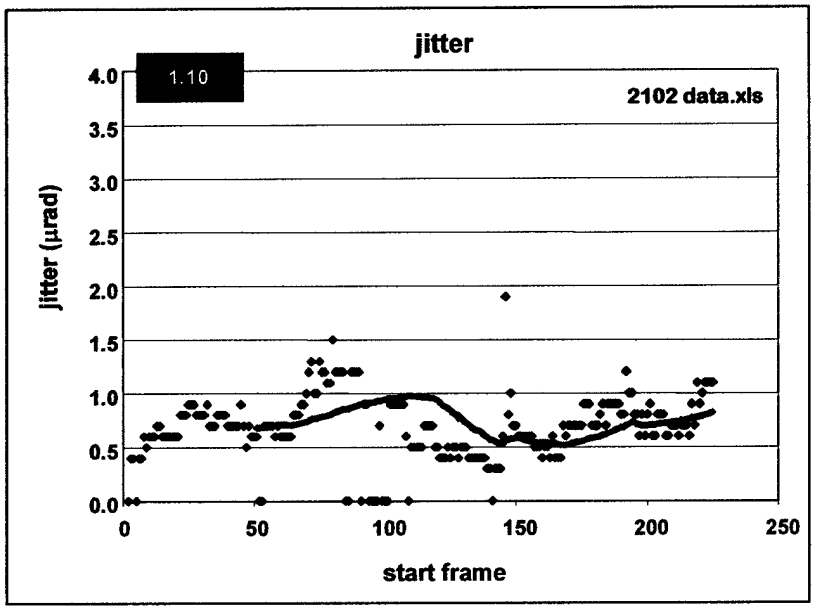

Figure 17. This figure shows analysis of pointing jitter from an AIT illumination of satellite 2102 during AIT. In this example a 50 point moving average is displayed. Each dot represents an estimate based on 25 shots, with the first displayed at shot#1.

If jitter is a primary concern during an experiment, the RHINO user may display the data in Figure 17 dynamically as part of a multiple window display.

Example 2. Boresight Dynamic Display with 50 Point Moving Average

Boresight (Section 5.1.2) is potentially a large source of error for an experiment. The dynamic display of boresight during a satellite engagement could alert an operator that, for example, time-of-flight lead ahead was failing to operate properly or that the system potentially had a systematic boresight error from an optics alignment error.

Early in during AIT, Nukove's boresight estimates, provided to the experimenters generally within 24 hours, showed a boresight estimated nearly 4-5µrad. It was quickly realized that this was caused by the tracker. The experiment was performed in terminator, that part of the day when the sun illuminates the target but the ground site is dark. Because of the solar illumination at nearly 90° relative to the ground-satellite angle, the tracker was following an edge of the target, thus the pointing was skewed by the half the length of the target. Corrective action was taken resulting in lowered boresight. Having such data available during a satellite pass could prove very valuable to the experimenters.

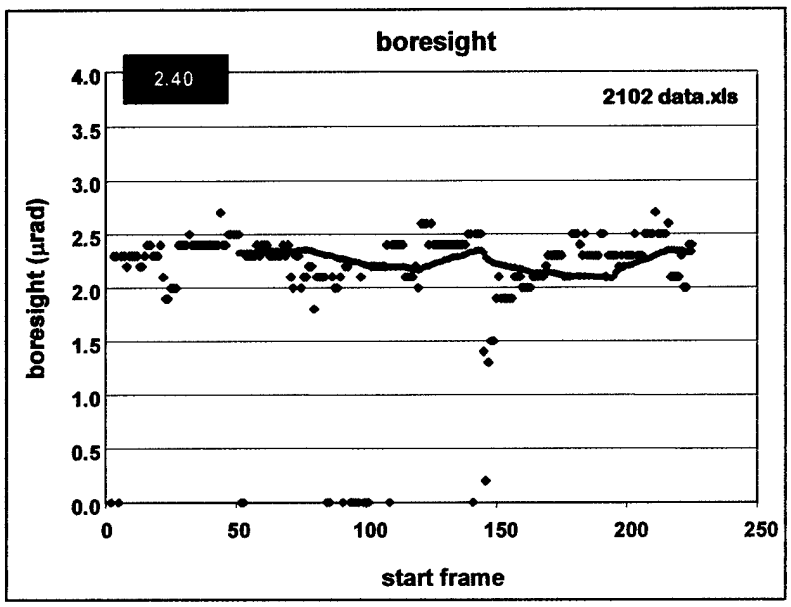

Figure 18. This figure contains all the same elements that Figure 17 contains, but displays the boresight estimate for 25 shots (dots) and the 50 point running estimate.

Figure 18 shows an example for satellite 2102 during AIT. In this example, with a beam FWHM≈3.5μrad, the boresight estimate is close to the budget set for AIT pointing.

Example 3. Numerical Display of Running Estimates

Figure 19 requires a detailed, column by column, explanation. The data used is a subset of the data that is used in both Figure 17 and Figure 18.

The first column shows 25 point sequential data sets (e.g. 45-69, 46-70…63-87). The second and third columns display the jitter and boresight estimates for a specific model (in this case Model 1 – see Figure 8). For each 25 point sequence the values would be available to an experiment.

The fourth column shows an estimate of the target optical cross section. While not a subject of the Phase I effort, Nukove has developed a technique for on-the-fly *OCS* estimates and these, too, may be displayed dynamically. The fifth column shows the statistical confidence Q associate with the χ^2 technique. For this example the minimum acceptable Q was set at 60% and estimates of jitter and boresight that resulted in Q<60% were discarded and are shown as zero on the jitter and boresight graphs. In this example, the pointing estimates from shots 51-75 and 52-76 were discarded.

The sixth and seventh columns show the fifty point running averages for jitter and boresight, respectively. One point requires explanation: When a 50 point set of estimates contains drop-outs due to low Q the running average simply dismisses the estimate. Thus in the example shown a 50 point average may in fact be a 48 point average. The setting for the cutoff Q will be the subject of Phase II efforts.

frames	j #1	b #1	OCS #1	max Q #1	j1 moving av	b1 moving av
45 69	0.70	2.40	1.29	98.2%		
46 70	0.50	2.50	1.34	93.8%		
47 71	0.70	2.50	1.34	98.2%		
48 72	0.60	2.50	1.34	87.8%		
49 73	0.60	2.50	1.73	98.2%		
50 74	0.60	2.50	1.73	87.8%	0.681	2.329
51 75				59.2%	0.681	2.329
52 76				59.2%	0.687	2.330
53 77	0.70	2.30	0.83	66.3%	0.694	2.330
54 78	0.70	2.30	0.83	66.3%	0.694	2.329
55 79	0.70	2.30	0.92	87.8%	0.700	2.329
56 80	0.70	2.30	0.92	87.8%	0.706	2.329
57 81	0.60	2.40	1.01	93.8%	0.706	2.333
58 82	0.70	2.30	1.01	98.2%	0.710	2.333
59 83	0.60	2.40	1.07	98.2%	0.710	2.335
60 84	0.60	2.40	1.07	98.2%	0.710	2.338
61 85	0.60	2.40	1.01	93.8%	0.710	2.340
62 86	0.60	2.30	1.01	98.2%	0.708	2.342
63 87	0.60	2.30	1.01	98.2%	0.706	2.344

Figure 19. This chart, available as a window under Phase I RHINO, shows data available for an operator. As such data is numerical and real-time; it can be ported to the telescope system as desired. A detailed discussion is given in the text.

Example 4. Bin Model Data

Figure 20 shows a subset of the actual analysis page in RHINO. In practice it would not be useful during an engagement. Some explanation is warranted.

Jitter	1.90	1.90	1.90	1.90	1.90	1.90	1.90
Boresight	2.10	2.20	2.30	2.40	2.50	2.60	2.70
Bin 1	1.59E-02	1.48E-02	1.37E-02	1.26E-02	1.16E-02	1.08E-02	9.89E-03
Bin 2	1.58E-01	1.37E-01	1.16E-01	9.70E-02	8.01E-02	6.47E-02	5.07E-02
Bin 3	4.45E-01	4.19E-01	3.88E-01	3.55E-01	3.29E-01	2.97E-01	2.69E-01
Bin 4	7.72E-01	7.54E-01	7.34E-01	7.16E-01	6.95E-01	6.71E-01	6.48E-01
Bin 5	1.00E+00	1.00E+00	1.00E+00	1.00E+00	1.00E+00	1.00E+00	1.00E+00
Bin 1 obs value	1	1	1	1	1	1	1
Bin 2 obs value	6	6	6	5	3	3	3
Bin 3 obs value	9	8	7	8	9	6	4
Bin 4 obs value	5	5	6	6	7	10	12
Bin 5 obs value	4	5	5	5	5	5	5
More	0	0	0	0	0	0	0
Q	0.146842388	0.267384882	0.354570107	0.267384882	0.091578194	0.05629028	0.007295056
chi_square	6.8	5.2	4.4	5.2	8	9.2	14
Jitter	2.40	2.40	2.40	2.40	2.40	2.40	2.40
Boresight	1.60	1.70	1.80	1.90	2.00	2.10	2.20
Bin 1	1.41E-02	1.31E-02	1.24E-02	1.14E-02	1.08E-02	9.81E-03	9.23E-03
Bin 2	1.52E-01	1.34E-01	1.25E-01	1.11E-01	9.83E-02	8.64E-02	7.53E-02
Bin 3	4.45E-01	4.22E-01	4.13E-01	3.94E-01	3.73E-01	3.54E-01	3.42E-01
Bin 4	7.70E-01	7.55E-01	7.50E-01	7.36E-01	7.22E-01	7.15E-01	7.07E-01
Bin 5	1.00E+00	1.00E+00	1.00E+00	1.00E+00	1.00E+00	1.00E+00	1.00E+00
Bin 1 obs value	1	1	1	1	1	1	1
Bin 2 obs value	6	6	6	6	5	4	3
Bin 3 obs value	9	8	8	8	8	8	9
Bin 4 obs value	5	5	5	5	6	7	7
Bin 5 obs value	4	5	5	5	5	5	5
More	0	0	0	0	0	0	0
Q	0.146842388	0.267384882	0.267384882	0.267384882	0.267384882	0.199148273	0.091578194
chi_square	6.8	5.2	5.2	5.2	5.2	6	8

Figure 20. This figure shows the working section of RHINO and likely would not be displayed during an engagement but used after-the-fact. Details are described in the text.

Two portions are shown in the top and bottom boxes. The bin models are for a beam FWHM = 3.5μrad, with a circular target of diameter 1.5μrad. The first and second rows show the jitter and boresight levels (in units of μrad) for bin analysis. For the upper box the jitter is 1.9 and the boresight increments from 2.10 to 2.70.

The next five rows show the bin endpoints (see Section 5.2) for each pointing hypothesis. Below those five rows are the actual counts within each bin for 25 simulated data points. A perfect match would result in bin counts all equal to five. In the example shown there is clearly no good match for this subset of analysis. This is reflected in both the value of Q and the value of χ^2.

Example 5. Sample of RHINO Analysis and Jitter/Boresight Display

An alternative dynamic display is also available. The jitter and boresight Q values associated with the χ^2 analysis are maintained in a graphics window, although would not be useful during an engagement. Figure 21 shows a subset of Q data. The highest value of Q occurs at $j = 0.80$ and $b = 2.20$. Surrounding the highest Q are estimates that fall away, reflecting the nature of the χ^2 test.

Jitter(row)/Boresight (col)	2.0000	2.1000	2.2000	2.3000	2.4000
0.0000	0%	0%	0%	0%	0%
0.1000	0%	0%	0%	0%	0%
0.2000	0%	0%	0%	0%	0%
0.3000	0%	0%	1%	0%	9%
0.4000	1%	1%	27%	52%	41%
0.5000	1%	41%	88%	74%	74%
0.6000	27%	59%	88%	88%	74%
0.7000	31%	59%	88%	88%	74%
0.8000	31%	59%	94%	74%	27%
0.9000	31%	74%	66%	74%	27%
1.0000	31%	59%	35%	20%	20%
1.1000	35%	66%	13%	20%	20%
1.2000	17%	35%	20%	20%	20%
1.3000	35%	3%	20%	20%	7%
1.4000	3%	20%	20%	7%	7%
1.5000	8%	20%	7%	7%	7%
1.6000	20%	7%	7%	7%	2%
1.7000	7%	7%	11%	9%	1%

Figure 21. This figure shows a subset of the calculated values of Q using the tool shown in Example 4. Jitter values are shown in the rows (0.000 – 1.700) and boresight models are shown in the columns. This example shows a good match, with an acceptable value of Q providing the best estimate of pointing.

As an alternative to the running displays (Figure 9 through Figure 11) is to display of the values of Q on a two dimensional grid. While this can be visually useful and displayed dynamically, the running averages have not been implemented.

Figure 22 shows an example from the full data set in Figure 21. When working with RHINO in real-time, the contour plot display is dynamic with estimates provided for data points 1-25, 2-26… etc. The graphic reflects the Q cutoff at 50% and the contours are in increments of 10% from 50% to 100%.

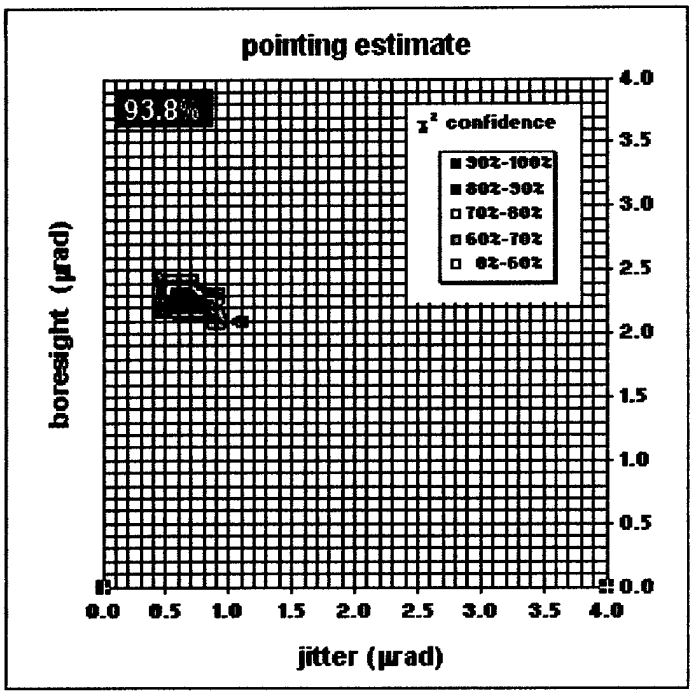

Figure 22. This contour shows one example of a 25 point data set analysis, with the jitter on the x-axis and the boresight on the y-axis. The highest confidence Q is 93.8% at $j = 0.80$ and $b = 2.20$.

References

1. G. Lukesh, S. Chandler and D.G. Voelz, "Estimation of laser system pointing performance by use of statistics of return photons," Appl. Opt. **39**, 1359-1371, 2000.
2. E. Caudill, G. Lukesh, R. Smith, S. Chandler, D. Voelz and K. Bush, "Satellite Laser Cross Sections From The Floodbeam Experiments", report, AFRL-DE-PS-TR-1998-1053, Air Force Research Laboratory, Kirtland AFB, NM, 1998.
3. G. Lukesh, S. Chandler and L. Cuellar, "Active Imaging Testbed: Radiometry and Satellite Optical Cross Section Estimation", AFRL-DE-TR-2001-1006, Air Force Research Laboratory, Kirtland AFB, NM (2001).
4. S. Chandler, G. Lukesh, S. Basu, D. Voelz, and J. Sjogren, "Model-based Beam Control for Illumination of Remote Objects – Part I: Theory and Real-Time Feasibility", *to appear,* Proceedings SPIE, Denver 2004 5552-13.
5. S. Basu, D. Voelz, S. Chandler, G. Lukesh, and J. Sjogren, "Model-based Beam Control for Illumination of Remote Objects – Part II: Laboratory Experiment", *to appear,* Proceedings SPIE Denver 2004 5552-14.
6. S. Chandler, G. Lukesh, D. Voelz, S. Basu, and J. Sjogren, "Model-based Beam Control for Illumination of Remote Objects", *to appear,* Proceedings SPIE International Conference on Remote Sensing, Gran Canaria, Spain, September 2004 5572-17.
7. J. Goodman, *Introduction to Fourier Optics*, 2nd Ed., McGraw-Hill,1996.
8. W. H. Press, S. A. Teukolsky, W. T. Vetterling, and B. P.Flannery, *Numerical Recipes in FORTRAN: The Art of Scientific Computing, 2nd ed.*, Cambridge University Press, Cambridge, 1992.
9. G. Lukesh and S. Chandler, "Non-imaging active system determination of target shape through a turbulent medium", Proceedings of the EOS/SPIE Symposium on Remote Sensing **4167,** September 2000, p. 111-119.